ACS Catalysis

Research Article

pubs.acs.org/acscatalysis

Electrocatalysis of Ethanol on a Pd Electrode in Alkaline Media: An *in Situ* Attenuated Total Reflection Surface-Enhanced Infrared Absorption Spectroscopy Study

Yao-Yue Yang,[†] Jie Ren,[‡] Qiao-Xia Li,[§] Zhi-You Zhou,*[,‡] Shi-Gang Sun,[‡] and Wen-Bin Cai*[,†]

[†]Shanghai Key Laboratory of Molecular Catalysis and Innovative Materials, Collaborative Innovation Center for Energy Materials, Department of Chemistry, Fudan University, Shanghai 200433, China

[‡]State Key Laboratory of Physical Chemistry of Solid Surfaces, Department of Chemistry, College of Chemistry and Chemical Engineering, School of Energy Research, Xiamen University, Xiamen 361005, China

[§]College of Environmental and Chemical Engineering, Shanghai University of Electric Power, Shanghai 200090, China

Supporting Information

ABSTRACT: *In situ* attenuated total reflection surface-enhanced infrared absorption spectroscopy in conjunction with H−D isotope replacement is used to investigate the dissociation and oxidation of CH_3CH_2OH on a Pd electrode in 0.1 M NaOH, with a focus on identifying the chemical nature of the pivotal intermediate in the so-called dual-pathway (C1 and C2) reaction mechanism. Real-time spectroelectrochemical measurements reveal a band at ~1625 cm^{-1} showing up prior to the multiply bonded CO_{ad} band. CH_3CD_2OH and D_2O are used to exclude the spectral interference with this band from interfacial acetaldehyde and H_2O, respectively, confirming for the first time that the ~1625 cm^{-1} band is due to the adsorbed acetyl on the Pd electrode in alkaline media. The spectral results suggest that the as-adsorbed acetyl (CH_3CO_{ad}) is oxidized to acetate from approximately −0.4 V as the potential moves positively to conclude the C2 pathway. Alternatively, in the C1 pathway, the CH_3CO_{ad} is decomposed to α-CO_{ad} and β-CH_x species on the Pd electrode at potentials more negative than approximately −0.1 V; the α-CO_{ad} species is oxidized to CO_2 at potentials more positive than approximately −0.3 V, while the β-CH_x species may be first converted to CO_{ad} at approximately −0.1 V and further oxidized to CO_2 at more positive potentials.

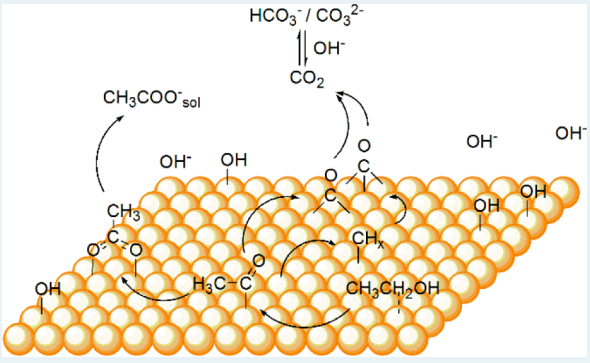

KEYWORDS: *Pd electrode, ethanol, electrocatalysis, alkaline media, surface-enhanced infrared spectroscopy, mechanism*

1. INTRODUCTION

Alkaline direct ethanol fuel cells (ADEFCs) are considered as a promising power source for automobile and portable applications,[1,2] for the following reasons. First, ethanol (CH_3CH_2OH) has merit as a fuel because of its high theoretical energy density, low price, biorenewability, and benign effect on the environment. More importantly, ADEFCs may overcome a major hurdle in large-scale commercialization of fuel cells, that is, the use of rare and expensive platinum (Pt) as the main catalyst,[3] because lower-cost palladium (Pd) exhibits a comparable electrocatalytic activity toward ethanol oxidation reaction (EOR) in alkaline media despite a poor activity in acidic media.[2,4]

In fact, Pd-based catalysts for EOR have been synthesized, including but not limited to Pd nanocrystals,[5,6] a Pd−metal oxide composite, and Pd-based alloy catalysts.[7−12] However, their performance for EOR needs to be further upgraded to meet the requirements of ADEFCs of the next generation.[1−3,7] The road map to new powerful Pd-based catalysts is to first obtain a good understanding of EOR on the Pd electrode in alkaline media at the molecular level, which has already been demonstrated in the pursuit of Pt-based catalysts in acidic media.

So far, the so-called dual-pathway (C1 and C2) mechanism for EOR[13−26] has been proposed because of the intensive studies of the Pt electrode in acidic media as shown in Scheme 1, despite the controversy over the details. According to this mechanism, acetaldehyde forms at lower potentials that can be readily oxidized to acetate as an incomplete oxidation product; alternatively, ethanol or acetaldehyde may decompose to CO_{ad}

Scheme 1. Dual-Pathway Mechanism Suggested for Ethanol Oxidation at a Pt Electrode in Acidic Media

$CH_3CH_2OH \rightarrow CH_3CHO \rightarrow CH_3COOH$ C2 Pathway

$CO + Fragments \rightarrow CO_2$ C1 Pathway

Received: December 16, 2013
Revised: January 20, 2014
Published: January 27, 2014

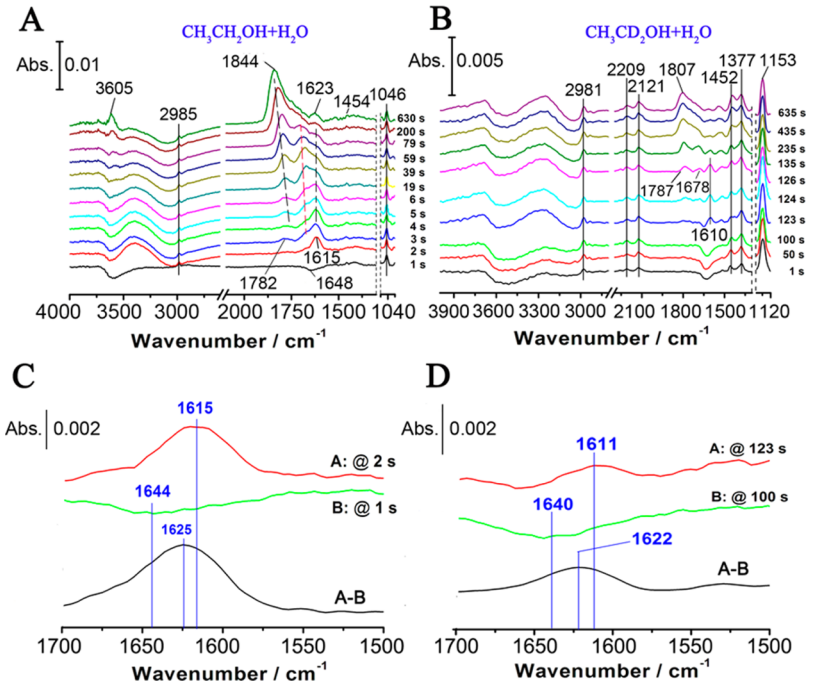

Figure 1. Real-time ATR-SEIRA spectra on a Pd electrode in 0.5 M CH_3CH_2OH with a 0.1 M $NaOH/H_2O$ solution (A) or 0.5 M CH_3CD_2OH with a 0.1 M $NaOH/H_2O$ solution (B). Locally amplified spectra for spectra at 1 and 2 s in panel A (C) and spectra at 100 and 123 s in panel B and their subtracted spectra (marked by A − B) (D). The single-beam spectrum recorded in a neat $NaOH/H_2O$ solution was used as the reference spectrum.

and CH_x species via the cleavage of its C−C bond and eventually be oxidized to CO_2 at higher potentials.

However, it is not clear whether or to what extent the mechanism proposed for EOR on Pt in acidic media may be extended for EOR on a Pd electrode in basic media because there have been far fewer *in situ* investigations of the latter. Experimentally, electrochemical methods,[6,27] high-performance liquid chromatography (HPLC),[28] and differential electrochemical mass spectroscopy[29] were applied to probe the pertinent reaction, providing indirect (not at the molecular level) or online (*ex situ*) information of solution species, including acetate or acetaldehyde species. Fortunately, *in situ* surface spectroscopic studies can identify intermediates for EOR on the Pd electrode. By using external infrared reflection absorption spectroscopy (IRAS) with a thin-layer configuration, Fang et al.[30] measured the pH-dependent EOR product, and we[31] also evaluated the selectivity of the reaction products (i.e., CO_2 and acetate) as a function of potential. Nevertheless, IRAS is not sufficiently sensitive to probe low-coverage or weakly adsorbed intermediates to provide real-time mechanistic insight.[32] In contrast, attenuated total reflection surface-enhanced infrared absorption spectroscopy (ATR-SEIRAS) permits high surface sensitivity and unobstructed mass transport[33−35] and thus is promising for the disclosure of more details about the surface EOR process on Pd in alkaline media as already demonstrated in the case of methanol oxidation.[36]

On the other hand, the open circuit condition is always encountered in fuel cell studies, and self-dissociation of a fuel molecule at the open circuit potential (OCP) is usually a prelude or starting point to its electrocatalytic oxidation. A well-known example is that formic acid decomposes to form CO_{ad} species on a Pt electrode[37−40] through dehydration at OCP, which can be oxidized only at much higher potentials and thus prevents the dehydrogenation of FA at lower potentials. Also, as we demonstrated before, methanol can readily self-dissociate on a Pd electrode in alkaline media, and the as-generated CO_{ad} species is a reaction intermediate in methanol electro-oxidation at higher potentials.[36] Along this line, to arrive at an improved understanding of the EOR, it is necessary to explore ethanol self-dissociation occurring on the Pd electrode at OCP.

In this work, electrochemical ATR-SEIRAS is applied to investigate the dissociation and oxidation of CH_3CH_2OH on Pd surfaces in alkaline media, aiming to clarify the reaction mechanism with a focus on the pivotal intermediate species pertinent to the EOR on Pd electrode.

2. EXPERIMENTAL SECTION

The Pd film working electrode on the reflecting plane of a Si prism was prepared according to the so-called "two-step wet process", which has been described previously in detail.[36,41] The Si prism with the Pd film on was assembled into a spectroelectrochemical cell that was then fixed in a homemade optics system built in the chamber of a Varian FT3000 infrared spectrometer (Varian Inc.) for electrochemical ATR-SEIRAS measurements at an incidence angle of ∼65°. Unless otherwise stated, the spectra recorded in a neat 0.1 M $NaOH/H_2O$ (or D_2O) solution and CH_3CH_2OH (or CH_3CD_2OH)-containing 0.1 M $NaOH/H_2O$ (or D_2O) solution were used as the reference and sample spectra, respectively. All ATR-SEIRAS spectra are given in absorbance units defined as $-\log(I/I_0)$, where I and I_0 represent the sample and reference single-beam spectra, respectively. Unless otherwise stated, the acquisition time for each single-beam spectrum in a real-time measurement is 1 s (approximately six interferograms) at a spectral resolution of 8 cm^{-1}. A CHI 660 electrochemistry workstation (CH Instruments, Inc.) was used to measure the open circuit potential (OCP) and to control the electrode potential. A Pt sheet and a saturated calomel electrode (SCE) were used as the counter and reference electrodes, respectively. All chemicals,

dx.doi.org/10.1021/cs401198t | ACS Catal. 2014, 4, 798−803

including D_2O (99.9% D, Cambridge Isotope Laboratories, Inc.) and deuterated ethanol (99.9% D, Cambridge Isotope Laboratories, Inc.), were used without further purification. All H_2O solutions were prepared with Millipore Milli-Q water (≥18.2 Ω cm) and deareated by being bubbled with high-purity N_2 for at least 1 h.

3. RESULTS AND DISCUSSION

3.1. Self-Dissociation of Ethanol. Panels A and B of Figure 1 show real-time ATR-SEIRAS spectra on a Pd electrode at OCP after the electrolyte was changed from neat 0.1 M NaOH to CH_3CH_2OH and CH_3CD_2OH-containing 0.1 M NaOH solutions, respectively, at time zero. It can be seen that a downward band at 1648 cm^{-1} showed up immediately, which can be attributed to an exclusion of interfacial H_2O by incoming CH_3CH_2OH (or CH_3CD_2OH). The term "interfacial species" in this work refers to the species on the surface and close to the surface in the double-layer region. In response, vibrational bands corresponding to interfacial CH_3CH_2OH or CH_3CD_2OH were observed at ~2980, ~2120, ~2209, ~1377, ~1452, ~1153, and ~1046 cm^{-1} within 1 s (see Table 1 for the band assignments), while the broad band at ~3400 cm^{-1} should be associated with the O−H stretching vibration of interfacial ethanol and water.[15,19,30,31] Later, the band of multiply/doubly bonded CO_{ad} species arising from the ethanol dissociation appeared at ~1671 cm^{-1}, and its intensity increased with a gradual frequency shift to ~1844 cm^{-1}, the dissociation rate of which differs between CH_3CH_2OH and CH_3CD_2OH because of the so-called H−D kinetic isotope effect (KIE), as also reflected from the variation of the OCP versus time (Figure S1 of the Supporting Information).

Table 1. Band Assignments in Figures 1 and 2

band frequency (cm^{-1})	assignment
3605	ν(OH) of free water[42,49]
2981, 2900	ν(C−H) of CH_3CH_2OH[15,19,26]
2660 (downward)	ν(OD) of D_2O[44]
2209, 2120	ν(C−D) of CH_3CD_2OH[50]
1671−1844	$\nu(CO_{ad})$ of CO_{ad} species[16,31,36,41,42]
1648 (downward)	δ(HOH) of interfacial H_2O[44]
1610−1640	ν(C═O) of adsorbed acetyl[19,22,25]
1452, 1391	δ(C−H) of CH_3CH_2OH[15,22,26]
1153	ν(C−OH) of CH_3CD_2OH[50]
1046	ν(C−OH) of CH_3CH_2OH[31]

In panels A and B of Figure 1, an upward 1610−1640 cm^{-1} band emerged sometime after the replacement of the electrolyte. The band frequency apparently red-shifts because of its overlap with the δ(HOH) band of interfacial water (~1640 cm^{-1} downward). To minimize the spectral interference, a spectral subtraction was made by taking a ratio of spectrum A to spectrum B, leading to a band frequency shift from 1615 to 1625 cm^{-1} in Figure 1C and from 1611 to 1622 cm^{-1} in Figure 1D. In other words, this band should be centered at ~1625 ± 4 cm^{-1} in consideration of a spectral resolution of 8 cm^{-1} in the measurement. According to our previous measurement,[36] the lowest vibrational frequency for multiply coordinated CO (CO_M) on a Pd electrode in 0.1 M NaOH at −0.70 V (SCE) was located at a frequency of >1660 cm^{-1}. Hence, this 1625 cm^{-1} band should not be assigned to the $\nu(CO)_M$ band, because the latter (if any) should have a frequency of >1660 cm^{-1} at −0.55 V [the OCP (see Figure S1 of the Supporting Information)] considering the potential-induced frequency blue shift.[42] In fact, the frequency for the CO_M species is marked with a red dashed line in Figure 1A. Therefore, the 1625 cm^{-1} band could be reasonably ascribed to surface acetaldehyde or acetyl arising from ethanol dissociation.[22]

To distinguish between adsorbed acetaldehyde and acetyl, an ATR-SEIRAS measurement was also taken on a Pd electrode in a CH_3CD_2OH-containing alkaline solution. Note that the deuteration on α-H should have caused a significant red shift of the band frequency for adsorbed acetaldehyde species if any. However, as shown in Figure 1, the band frequency of 1625 ± 4 cm^{-1} derived from simple deconvolution is virtually unaffected within measurement error (see the band at 1631 ± 4 cm^{-1} at 6 s in Figure 2), demonstrating that this adsorbed intermediate species would be better assigned to acetyl than to acetaldehyde.

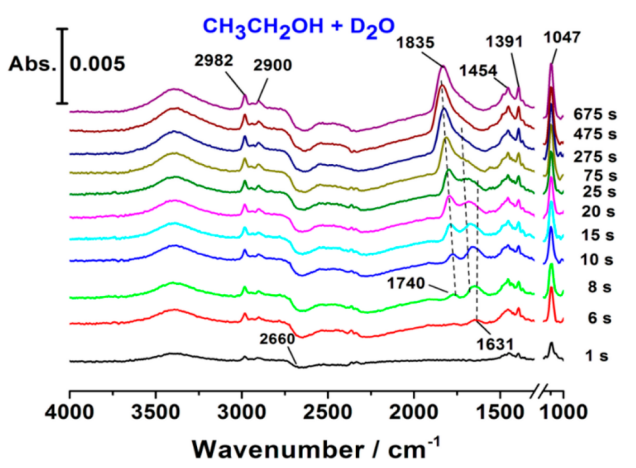

Figure 2. Real-time ATR-SEIRA spectra on a Pd electrode in 0.5 M CH_3CH_2OH with a 0.1 M $NaOH/D_2O$ solution. The single-beam spectrum recorded in a neat $NaOH/D_2O$ solution was used as the reference spectrum.

To further exclude the spectral interference from interfacial water, the ATR-SEIRAS measurement was taken using 0.5 M CH_3CH_2OH with a 0.1 M $NaOH/D_2O$ solution as the electrolyte instead, recalling that δ(DOD) and δ(HOD) (if any D−H exchange occurs[43]) are centered at 1206 and 1450 cm^{-1}, respectively.[44] As shown in Figure 2, a 1630 cm^{-1} band remained indeed, which can be attributed to the C═O stretching vibration of adsorbed acetyl [simplified as $\nu(C{=}O)_{acetyl}$ hereafter]. Notably, Shao et al.[25] and Heinen et al.[19] in their work on EOR at a Pt electrode in an acidic solution detected an IR band ranging from 1610 to 1640 cm^{-1} and assigned it to acetaldehyde and/or acetyl, though they did not elaborate on the uncertainty of the assignment of this band caused by a possible overlap of an interfacial water band.

During the whole dissociation process, adsorbed acetyl was observed earlier than CO_{ad} species (Figures 1 and 2), and the band intensity of adsorbed acetyl gradually diminished, which was accompanied by increasing CO_{ad} coverage. These observations suggest that surface ethanol first turns into adsorbed acetyl through fast dehydrogenation on α-C (within 1 s) at the Pd electrode, and the as-generated acetyl successively dissociates to α-CO_{ad} and carbonaceous fragments (β-CH_x) by C−C bond cleavage (*vide infra*), which is also favorable in terms of reaction energy barriers according to DFT calculations.[45−47] The dissociation rates for CH_3CH_2OH and

dx.doi.org/10.1021/cs401198t | ACS Catal. 2014, 4, 798−803

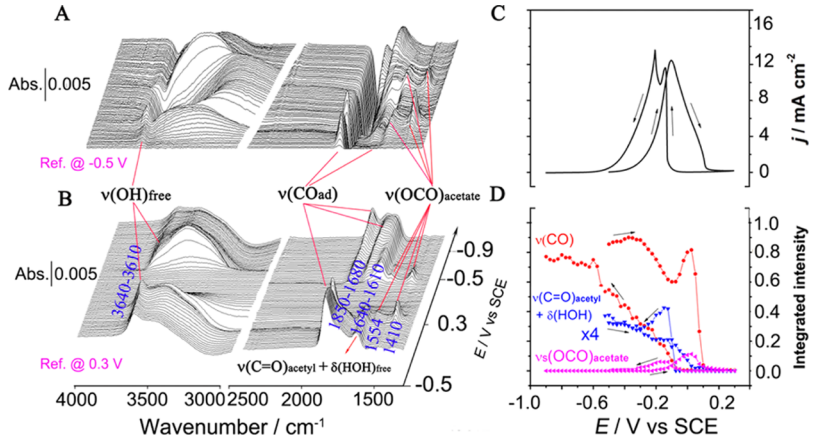

Figure 3. *In situ* ATR-SEIRA spectra obtained with a time resolution of 5 s on a Pd electrode in 0.1 M NaOH/0.5 M CH_3CH_2OH solution, taking the single-beam spectrum at −0.5 V (A) and 0.3 V (B) as the reference spectrum. (C) Corresponding cyclic voltammogram of the Pd electrode in a 0.1 M NaOH/0.5 M CH_3CH_2OH solution at 5 mV/s, together with (D) potential-dependent band intensities for $\nu(CO_{ad})$ (red), $\nu_s(OCO)$ of adsorbed acetate (pink), and $\nu(C{=}O)_{acetyl}$ + $\delta(HOH)_{free}$ (blue).

CH_3CD_2OH are quite different; as shown in Figure 1A, it takes only 1 s to produce adsorbed acetyl species for CH_3CH_2OH but around 120 s for CH_3CD_2OH (refer also to the OCP vs time profiles in Figure S1 of the Supporting Information). Meanwhile, the band intensity of CO_{ad} species in Figure 1B is distinctly lower than that in Figure 1A, suggestive of a higher coverage of CO_{ad} species at the Pd electrode in a CH_3CH_2OH-containing $NaOH/H_2O$ solution. Obviously, this is in accordance with a significant H−D KIE, as further described in the Supporting Information (see Figure S2 and the text). The KIE result also indicates that dehydrogenation of α-C-H rather than β-C-H occurs initially for EOR at the Pd electrode in alkaline media. For more details regarding the KIE on electrochemical measurements, please see ref 48.

3.2. Electro-oxidation of Ethanol. Shown in Figure 3 are potentiodynamic ATR-SEIRA spectra for EOR at the Pd electrode recorded as the potential was swept positively from the stable OCP around −0.5 V (SCE), using a single-beam spectrum recorded at −0.5 V (Figure 3A) or 0.3 V (Figure 3B) as the reference spectrum. On the basis of previous reports,[13,15,19,30,31,46] 1410 and 1554 cm^{-1} bands can be attributed to $\nu_s(OCO)$ of bridge-bonded acetate and $\nu_{as}(OCO)$ of solution acetate, respectively; the 1354 cm^{-1} band is assigned to the in-plane bending vibrations of the -CH_3 group of the adsorbed acetate [$\delta(CH_3)$], and the 1671−1844 cm^{-1} band is due to CO_{ad} species [$\nu(CO_{ad})$]. As discussed in section 3.1, the $\nu(C{=}O)_{acetyl}$ vibration is mainly responsible for the observed 1610−1640 cm^{-1} band, in addition to a minor contribution from $\delta(HOH)_{free}$ of interfacial water, given the single-beam spectrum acquired at 0.3 V in the same solution that was used for the reference spectrum.[22,49] The use of D_2O as the alternative solvent in this measurement could distort the real reaction kinetics because of the KIE when the potentiodynamic spectra were collected, although it is expected to remove the minor contribution from $\delta(HOH)_{free}$. Therefore, we take herewith the 1610−1640 cm^{-1} band [deconvuluted from the broad band consisting partly of the contribution from $\nu(CO)_M$ (see Figure S3 of the Supporting Information for the peak-fitting process)] to approximately represent the surface acetyl band and plot its intensity as a function of potential as shown in Figure 3D, in a simplified manner similar to the treatment of previously published data.[36,51] Meanwhile, we also show the potential-dependent intensities of the CO_{ad} and acetate bands in Figure 3D.

As shown in the cyclic voltammogram (Figure 3C), the ethanol oxidation was initialized at approximately −0.4 V at the Pd electrode in the forward potential scan, similar to that at the Pt electrode in alkaline media.[15,20,52] Concomitantly, the $\nu(C{=}O)_{acetyl}$ band intensity gradually declined, and the $\nu_s(OCO)$ band intensity of adsorbed acetate increased from the same potential and decreased at potentials above approximately −0.08 V (Figure 3D). As for the $\nu(CO_{ad})$ band intensity, it slightly increased from −0.4 to −0.3 V and then decreased from −0.3 to −0.08 V. Interestingly, the band intensity increased again from approximately −0.08 V (approximately corresponding to the initial formation of surface Pd oxide) and diminished sharply at approximately 0.05 V. During the backward potential scan, the oxidation current started to increase at approximately −0.08 V because of the reduction of surface Pd oxide. In response, the surface acetyl, acetate, and CO_{ad} species showed up at largely the same potentials with the former two species presenting peak-shaped intensities and the latter increasing monotonically as the potential was scanned negatively. The essentially inactive acetate ions could be desorbed from the surface at sufficiently positive and negative potentials because of the competitive adsorption of O-containing species and CO_{ad} (and H) species, respectively. Moreover, the acetate band intensity largely traced the voltammogram, which may suggest a predominant share of the C2 pathway in the overall EOR (*vide infra*).

It is worthwhile to note that the aforementioned C1 and C2 pathways are often used to account for EOR on both Pt and Pd electrodes, with the C2 pathway being predominant.[2,11] Nevertheless, no consensus has been reached regarding the key intermediate involved on the Pt electrode. Specifically, Lai et al.[28,52] proposed that the key intermediate acetaldehyde can either diffuse into the solution or remain near the electrode surface for further conversion to acetic acid on Pt. Christensen et al.[15] assumed $CH_3CH(OH)O$-Pt at 1274 cm^{-1} was a key intermediate in the direct path to acetate on the Pt electrode. In contrast, on the Pd electrode, no other adsorbed C2 species other than acetyl and acetate have been detected by either IRAS[30] (only acetate) or our current ATR-SEIRAS (both acetyl and acetate). As mentioned above, the intensity of the $\nu(C{=}O)_{acetyl}$ band decreased with an increase in the intensity of the

dx.doi.org/10.1021/cs401198t | *ACS Catal.* 2014, 4, 798−803

ν_s(OCO) band from approximately −0.4 V in the forward potential scan. Therefore, the adsorbed acetyl can be regarded as the key intermediate for the C2 pathway on the Pd electrode in alkaline media, as illustrated in Scheme 2.

Scheme 2. Reaction Pathways for Interfacial CH_3CH_2OH at the Pd Electrode in Alkaline Media[a]

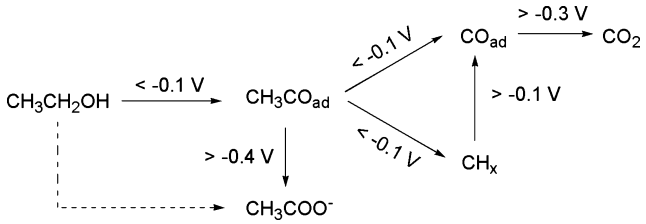

[a]The solid-line arrows denote the findings described in this work, while the dashed-line arrow denotes previously stated findings that were not accompanied by any direct spectral evidence.

Some details of the C1 pathway for EOR on the Pd electrode in alkaline media, especially the potential-dependent C−C bond cleavage and oxidation of CH_x fragments, should also be elucidated. Kutz et al.[16] and Souza-Garcia et al.[53] detected the bands associated with $\nu(^{12}CO_{ad})$ and $\nu(^{13}CO_{ad})$ in a $^{12}CH_3{}^{13}CH_2OH$-containing solution on Pt electrodes by using *in situ* SFG and IRAS techniques, respectively. Their isotopic spectroscopic investigations using ^{13}C-substituted ethanol strongly indicate the oxidation of carbonaceous fragments coming from the C−C bond cleavage to CO at rather high potentials,[16,53] laying a good basis for our discussions. In contrast, in section 3.1, we have used D-substituted ethanol to identify the chemical nature of the pivotal intermediate on the Pd electrode in alkaline media, i.e., to distinguish between the acetaldehyde and acetyl species. For this purpose, the use of $^{12}CH_3{}^{13}CH_2OH$ may not provide useful information.

It should be mentioned that no IR bands for CH_x have been clearly identified in the literature, because of the restriction of the surface selection rule and the overlapping of ethanol bands.[53] Only the Pt−C stretching band at ∼425 cm^{-1} was observed with surface-enhanced Raman spectroscopy (SERS) and assigned to the adsorbed CH_x species.[54] Unfortunately, such a low wavenumber cannot be accessible with electrochemical IR or SFG spectroscopy. Alternatively, the state of CH_x on the Pd electrode during the EOR in alkaline media may be deduced by the variation of the $\nu(CO_{ad})$ band intensity as a function of potential in this work, in analogy to that used in the treatment of SFG data.[16] As can be envisaged from the CO_{ad} band intensity variation with potential in Figure 3D, the CO_{ad} species is oxidized from approximately −0.3 V in the forward potential scan to form CO_2, and the rebound of the band intensity above approximately −0.08 V indicates that a new CO_{ad} species is generated. On the basis of the previous study,[16,20,53] the newly generated CO_{ad} at higher potentials in this work may be ascribed to the oxidation of surface β-CH_x species (see Scheme 2). As mentioned in section 3.1, the adsorbed acetyl species may decompose to α-CO_{ad} and β-CH_x species at OCP (approximately −0.55 V). The re-emergence of surface acetyl and CO_{ad} species at potentials below −0.08 V in the backward potential scan (Figure 3D) suggests that the dehydrogenation of ethanol and the further decomposition of acetyl could also occur at other lower potentials besides OCP. In other words, the C1 pathway for EOR involves an initial C−C bond cleavage at lower potentials to form α-CO_{ad} and β-CH_x species and subsequent oxidation of C1 species to CO_2 at sufficiently high potentials.

Notably, in the previous relevant investigation using IRAS,[30,31] only the solution acetate band and the very weak CO_{ad} band were barely identified, and no adsorbed acetyl band could be seen even with an extended spectral acquisition time because of the low surface sensitivity of IRAS, thereby preventing a spectrum-based understanding of the EOR mechanism on the Pd electrode in alkaline media. Nevertheless, this problem is circumvented via the application of *in situ* ATR-SEIRAS, which has provided more convincing evidence of the surface reaction intermediates (namely, adsorbed acetyl and CO_{ad} species) with a dependence on potential.

4. CONCLUSION

In summary, we have investigated the surface reaction of ethanol on Pd in alkaline media using ATR-SEIRAS and H−D isotope replacement on α-C to improve our understanding of the self-dissociation and oxidation processes relevant to the Pt-free anode of DEFCs. The real-time spectral measurements with and without isotope labeling indicate that ethanol may take dehydrogenation at α-C to form adsorbed acetyl rather than acetaldehyde, followed by a successive decomposition to C1 species, including CO_{ad} and CH_x at open circuit potential or lower potentials. As the potential becomes more positive, the adsorbed acetyl is a pivotal intermediate that may be converted to either acetate in the C2 pathway or CO_2 via the C1 species described above; adsorbed CH_x may also be converted to CO_{ad} species at high potentials. Thus, despite different intermediates, the reaction pathways for EOR on the Pd electrode in alkaline media are more or less similar to that on the Pt electrode in basic and acidic media. This study may provide a hint about the design of novel anode catalysts for DEFCs as it suggests that inhibiting direct oxidation of adsorbed acetyl should be effective for enhancing the C1 pathway of EOR.

■ ASSOCIATED CONTENT

Supporting Information

OCP versus time profiles for ethanol dissociation on Pd in NaOH, linear sweep voltammograms showing the H−D KIE for EOR on Pd in NaOH, and curve fitting of the selected bands over the range of 1550−1900 cm^{-1}. This material is available free of charge via the Internet at http://pubs.acs.org.

■ AUTHOR INFORMATION

Corresponding Authors

*E-mail: wbcai@fudan.edu.cn.
*E-mail: zhouzy@xmu.edu.cn.

Notes

The authors declare no competing financial interest.

■ ACKNOWLEDGMENTS

W.-B.C. is thankful for financial support from NSFC (21073045 and 21273046) and SMCST (11JC140200 and 08DZ2270500). Z.-Y.Z. acknowledges partial support from NSFC (21073152), and Q.-X.L. is thankful for the partial support from NSFC (21103107).

REFERENCES

(1) Rabis, A.; Rodriguez, P.; Schmidt, T. J. *ACS Catal.* **2012**, *2*, 864−890.
(2) Bianchini, C.; Shen, P. K. *Chem. Rev.* **2009**, *109*, 4183−4206.
(3) Brouzgou, A.; Song, S. Q.; Tsiakaras, P. *Appl. Catal., B* **2012**, *127*, 371−388.
(4) Antolini, E.; Gonzalez, E. R. *J. Power Sources* **2010**, *195*, 3431−3450.
(5) Zhang, H. X.; Wang, H.; Re, Y. S.; Cai, W. B. *Chem. Commun.* **2012**, *48*, 8362−8364.
(6) Ma, L.; Chu, D.; Chen, R. R. *Int. J. Hydrogen Energy* **2012**, *37*, 11185−11194.
(7) Wang, Y.; Shi, F.-F.; Yang, Y.-Y.; Cai, W.-B. *J. Power Sources* **2013**, *243*, 369−373.
(8) Du, W. X.; Mackenzie, K. E.; Milano, D. F.; Deskins, N. A.; Su, D.; Teng, X. W. *ACS Catal.* **2012**, *2*, 287−297.
(9) Shen, S. Y.; Zhao, T. S.; Xu, J. B.; Li, Y. S. *J. Power Sources* **2010**, *195*, 1001−1006.
(10) Xu, J. B.; Zhao, T. S.; Shen, S. Y.; Li, Y. S. *Int. J. Hydrogen Energy* **2010**, *35*, 6490−6500.
(11) Antolini, E. *Energy Environ. Sci.* **2009**, *2*, 915−931.
(12) Shen, P. K.; Xu, C. W. *Electrochem. Commun.* **2006**, *8*, 184−188.
(13) Figueiredo, M. C.; Santasalo-Aarnio, A.; Vidal-Iglesias, F. J.; Solla-Gullon, J.; Feliu, J. M.; Kontturi, K.; Kallio, T. *Appl. Catal., B* **2013**, *140*, 378−385.
(14) Li, M.; Liu, P.; Adzic, R. R. *J. Phys. Chem. Lett.* **2012**, *3*, 3480−3485.
(15) Christensen, P. A.; Jones, S. W. M.; Hamnett, A. *J. Phys. Chem. C* **2012**, *116*, 24681−24689.
(16) Kutz, R. B.; Braunschweig, B.; Mukherjee, P.; Dlott, D. D.; Wieckowski, A. *J. Phys. Chem. Lett.* **2011**, *2*, 2236−2240.
(17) Kim, I.; Han, O. H.; Chae, S. A.; Paik, Y.; Kwon, S. H.; Lee, K. S.; Sung, Y. E.; Kim, H. *Angew. Chem., Int. Ed.* **2011**, *50*, 2270−2274.
(18) Lai, S. C. S.; Koper, M. T. M. *J. Phys. Chem. Lett.* **2010**, *1*, 1122−1125.
(19) Heinen, M.; Jusys, Z.; Behm, R. J. *J. Phys. Chem. C* **2010**, *114*, 9850−9864.
(20) Lai, S. C. S.; Koper, M. T. M. *Phys. Chem. Chem. Phys.* **2009**, *11*, 10446−10456.
(21) Kowal, A.; Li, M.; Shao, M.; Sasaki, K.; Vukmirovic, M. B.; Zhang, J.; Marinkovic, N. S.; Liu, P.; Frenkel, A. I.; Adzic, R. R. *Nat. Mater.* **2009**, *8*, 325−330.
(22) Heinen, M.; Jusys, Z.; Behm, R. J. *ECS Trans.* **2009**, *25*, 259−269.
(23) Colmati, F.; Tremiliosi-Filho, G.; Gonzalez, E. R.; Berna, A.; Herrero, E.; Feliu, J. M. *Faraday Discuss.* **2008**, *140*, 379−397.
(24) Rao, V.; Hariyanto; Cremers, C.; Stimming, U. *Fuel Cells* **2007**, *7*, 417−423.
(25) Shao, M. H.; Adzic, R. R. *Electrochim. Acta* **2005**, *50*, 2415−2422.
(26) Iwasita, T.; Pastor, E. *Electrochim. Acta* **1994**, *39*, 531−537.
(27) Liang, Z. X.; Zhao, T. S.; Xu, J. B.; Zhu, L. D. *Electrochim. Acta* **2009**, *54*, 2203−2208.
(28) Santasalo-Aarnio, A.; Kwon, Y.; Ahlberg, E.; Kontturi, K.; Kallio, T.; Koper, M. T. M. *Electrochem. Commun.* **2011**, *13*, 466−469.
(29) Cantane, D. A.; Lima, F. H. B. *Electrocatalysis* **2012**, *3*, 324−333.
(30) Fang, X.; Wang, L. Q.; Shen, P. K.; Cui, G. F.; Bianchini, C. *J. Power Sources* **2010**, *195*, 1375−1378.
(31) Zhou, Z. Y.; Wang, Q. A.; Lin, J. L.; Tian, N.; Sun, S. G. *Electrochim. Acta* **2010**, *55*, 7995−7999.
(32) Osawa, M. In *Handbook of Vibrational Spectroscopy*; Chalmers, J. M., Griffiths, P. R., Eds.; John Wiley & Sons: Chichester, U.K., 2002; Vol. *1*, pp 785−799.
(33) Yang, Y. Y.; Zhang, H. X.; Cai, W. B. *J. Electrochem.* **2013**, *19*, 6−16.
(34) Griffiths, P. R. Surface-Enhanced Infrared Absorption: Principles and Applications. In *Spectroscopic Properties of Inorganic and Organometallic Compounds: Techniques, Materials and Applications*; Yarwood, J., Douthwaite, R., Duckett, S., Eds.; Royal Society of Chemistry: London, 2013; Vol. *44*, pp 95−122.
(35) Osawa, M. *Bull. Chem. Soc. Jpn.* **1997**, *70*, 2861−2880.
(36) Yang, Y. Y.; Ren, J.; Zhang, H. X.; Zhou, Z. Y.; Sun, S. G.; Cai, W. B. *Langmuir* **2013**, *29*, 1709−1716.
(37) Capon, A.; Parsons, R. *J. Electroanal. Chem.* **1973**, *44*, 1−7.
(38) Capon, A.; Parsons, R. *J. Electroanal. Chem.* **1973**, *44*, 239−254.
(39) Capon, A.; Parsons, R. *J. Electroanal. Chem.* **1973**, *45*, 205−231.
(40) Samjeske, G.; Miki, A.; Ye, S.; Yamakata, A.; Mukouyama, Y.; Okamoto, H.; Osawa, M. *J. Phys. Chem. B* **2005**, *109*, 23509−23516.
(41) Wang, J. Y.; Zhang, H. X.; Jiang, K.; Cai, W. B. *J. Am. Chem. Soc.* **2011**, *133*, 14876−14879.
(42) Yan, Y. G.; Yang, Y. Y.; Peng, B.; Malkhandi, S.; Bund, A.; Stimming, U.; Cai, W. B. *J. Phys. Chem. C* **2011**, *115*, 16378−16388.
(43) Pastor, E.; Iwasita, T. *Electrochim. Acta* **1994**, *39*, 547−551.
(44) Lappi, S. E.; Smith, B.; Franzen, S. *Spectrochim. Acta, Part A* **2004**, *60*, 2611−2619.
(45) Wang, E. D.; Xu, J. B.; Zhao, T. S. *J. Phys. Chem. C* **2010**, *114*, 10489−10497.
(46) Li, M.; Guo, W. Y.; Jiang, R. B.; Zhao, L. M.; Shan, H. H. *Langmuir* **2010**, *26*, 1879−1888.
(47) Cui, G. F.; Song, S. Q.; Shen, P. K.; Kowal, A.; Bianchini, C. *J. Phys. Chem. C* **2009**, *113*, 15639−15642.
(48) Ren, J.; Yang, Y.-Y.; Zhang, B.-W.; Tian, N.; Cai, W.-B.; Zhou, Z.-Y.; Sun, S.-G. *Electrochem. Commun.* **2013**, *37*, 49−52.
(49) Yan, Y. G.; Peng, B.; Yang, Y. Y.; Cai, W. B.; Bund, A.; Stimming, U. *J. Phys. Chem. C* **2011**, *115*, 5584−5592.
(50) Pinchas, S.; Laulicht, I. *Infrared Spectra of Labelled Compounds*; Academic Press: London, 1971.
(51) Zhou, Z. Y.; Tian, N.; Chen, Y. J.; Chen, S. P.; Sun, S. G. *J. Electroanal. Chem.* **2004**, *573*, 111−119.
(52) Lai, S. C. S.; Kleijn, S. E. F.; Ozturk, F. T. Z.; Vellinga, V. C. V.; Koning, J.; Rodriguez, P.; Koper, M. T. M. *Catal. Today* **2010**, *154*, 92−104.
(53) Souza-Garcia, J.; Herrero, E.; Feliu, J. M. *ChemPhysChem* **2010**, *11*, 1391−1394.
(54) Lai, S. C. S.; Kleyn, S. E. F.; Rosca, V.; Koper, M. T. M. *J. Phys. Chem. C* **2008**, *112*, 19080−19087.